HERSCHEL SPIRE

DPU AVM Design Description

Document Ref: SPIRE-IFS-PRJ-001389

Issue 1

Distribution List :

K. King		
B. Swinyard		
J. Delderfield		
E. Sawyer		
R. Cerulli		
S. Molinari		
G. Liu’		

Prepared by: Renato Orfei

Date: 8 October 2002

Document Status Sheet:

Document Title: Herschel SPIRE DPU AVM Design Description			
Issue	**Revision**	**Date**	**Reason for Change**
Issue 1		8 October 2002	First Issue

Document Change Record :

Document Title: Herschel SPIRE DPU AVM Design Description	
DOCUMENT REFERENCE NUMBER: SPIRE-IFS-PRJ-001389	
Document Issue/Revision Number: Issue 1	
Section	**Reason For Change**
All	Issue 1

1 INTRODUCTION

1.1 Scope of the document

The purpose of this document is to describe the AVM as compared to the other planned models. This document is part of the AVM EIDP.

1.2 Acronyms

AD	Architectural Design
ATP	Acceptance Test Plan
AVM	Avionic Model
BSW	Basic SW
CGS	Carlo Gavazzi Space
CIDL	Configuration Item Data List
CSL	Configuration Status List
CNR	Consiglio Nazionale delle Ricerche
CPP	Coordinated Parts Procurement
CPP	Coordinated Parts Procurement Board
CPU	Control Processing Unit
CDMS	Central Data Management System
CDMU	Central Data Management Unit

CQM	Cryogenic Qualification Model
DCU	Detector Control Unit
DDD	Detailed Design Document
DPU	Digital Processing Unit
EEPROM	Electrically Erasable Programmable Read Only Memory
EMC	Electro Magnetic Compatibility
EMI	Electro Magnetic Interference
ESA	European Space Agency
FIRST	Far InfraRed and Submillimeter Telescope
HK	HouseKeeping
HW	HardWare
IBDR	Instrument Baseline Design Review
ICD	Interface Control Document
ICDR	Instrument Critical Design Review
ICU	Instrument Control Unit
IHDR	Instrument Hardware Design Review
IFSI	Istituto di Fisica dello Spazio Interplanetario
ISVR	Instrument Science Verification Review
MCU	Mechanism Control Unit
NA	Not Applicable
OBS	On-Board Software
PA	Product Assurance
PDU	Power Distribution Unit

PROM	Programmable Read Only Memory
S/C	SpaceCraft
SCC	SpaceCraft Components
SCU	System Control Unit
SEU	Single Event Upset
SPIRE	Spectral and Photometric Imaging Receiver
S/S	SubSystem
SVM	Service Module
SW	Software
TBC	To Be Confirmed
TBD	To Be Defined
TBW	To Be Written
TV	Thermal Vacuum
WBS	Work Breakdown Structure

1.3 References

1.3.1 Applicable Documents

AD	Name
01	SPIRE Instrument Specification
02	Herschel/Planck Instrument Interface Document Part A
03	Herschel/Planck Instrument Interface Document, part B-Instrument SPIRE
04	DPU/ICU P.A.Plan
05	DPU/ICU OBS PA Plan

1.3.2 Reference Documents

Document Reference	Name	Reference
REF1	CPU Board Specification	DPU-SP-CGS-001 Issue 1
REF2	I/F Board Specification	DPU-SP-CGS-002 Issue 1
REF3	DC/DC Board Specification	DPU-SP-CGS-004 Issue 1
REF4	Mother Board Specification	DPU-SP-CGS-005 Issue 1
REF5	CPU Board Design	Herschel CPU Main EM1.DSN
REF6	CPU Board Piggy-Back Design	Herschel CPU DM PIGGY EM1.DSN
REF7	Interface Board Design	PSI-E000_0.00.DSN
REF8	DC/DC Converter Board Design	DC DC FIRST DESIGN1 EM.DSN
REF9	Mother-Board Design	MOTHERBOARD_2_D.DSN
REF10	DPU-BSW SOFTWARE REQUIREMENTS DOCUMENT	DPU-SQ-CGS-001 Issue 2
REF11	DPU-BSW SOFTWARE A.D. DOCUMENT	DPU-AD-CGS-001 Issue 1
REF12	Herschel SPIRE DPU OBS SSD	SPIRE-IFS-PRJ-001036 Draft 0.9
REF13	Herschel SPIRE DPU OBS URD	SPIRE-IFS-PRJ-000444 Issue 1.1
REF14	SPIRE OBS SVVP/Acceptance Plan	SPIRE-IFS-DOC-001392 Draft 0.5
REF15	Box Interface Control Drawing	SPIRE_DPU-Box5.pdf
REF16	DPU OBS Test Report	SPIRE-IFS-REP-001393 Issue 1

2 Design Description

The AVM unit is electrically, mechanically and thermally representative of the flight unit, but without redundancy. It makes use of standard commercial components. The DPU specifications as far as the hardware is concerned are described in REF1 to REF4, while the hardware design is described in REF5 to REF9.

The AVM software is described in REF10 to REF14.

The AVM OBS will be upgradable via EGSE and capable to test the S/C I/F and the available subsystems and or the subsystems simulators.

2.1 AVM Hardware Differences

The electrical design of the various models is just the same.

The hardware differences between the Avionic Model and the following models are:

- the quality level of components that are just commercial in the AVM;
- the depth of the 1553B Dual Port RAM (4 k x 16 Bit instead of 16 k x 16 Bit)
- the depth of the fast link FIFOs (4 k x 16 Bit instead of 8 k x 16 Bit).

2.2 AVM Software Differences

The AVM software, both the boot SW written in PROM and the Application Software written in EEPROM, is upgradable. The upgrade in a first moment will be done only through the JTAG connection on the CPU board, while later on the SW will be upgraded through the Telecommand link and the EGSE (SCOS 2000 and the CDMS).

The AVM software is fully representative of the FM software with the following exceptions that will be implemented before the EQM delivery:

- Burst Mode
- Patching
- Autonomy functions (requirements not yet received).

3 Thermal Analysis

3.1 Introduction

To simplify the analysis it is considered only the worst case so that all computations are made easy and there is no need of dedicated software programmes, with a lot of thermal data to be input in order to get in output a simulated temperature distribution and time evolution.

As the DPU is an electronic box located outside the cryostat we are also not interested in the temperature evolution of the different section/boards of the DPU after the switch-ON and the steady state thermal state is sufficient.

To our purposes it is important to check that no electronic component is used outside its rated temperature range, that for qualified components is - 55 °C to + 150 °C; in particular the hot side is to be verified, the cold side (-30 °C) being relevant only for the switch-ON properties. The DPU box operating temperatures are –15 °C to +45 °C; the switch-OFF temperature is +50 °C (AD3). This operating temperature is monitored at the foot interface between DPU and S/C and the S/C is responsible to keep it within the limits.

3.2 Rationale for the analysis

The thermal analysis of the DPU is restricted to the DC/DC converter board where there are the more thermally stressed components, that is the power FETs of the PWM that are switched ON and OFF by the PWM circuitry, and through which flows all the current drawn by the converter itself.

The following hypothesis are considered, taking into account a DC/DC conversion efficiency of 70% (REF4):

1. the total power required by the DPU is 24 W:
2. The total power of 24 W is divided in 16.8 W dissipated by the CPU and the I/F boards and 7.2 W dissipated by the DC/DC converter board. This 7.2 W and are managed by two power FETs. This is surely the worst case assumption as we neglect the power dissipated by

the rectifying diodes, chokes, transformers etc and we consider that all the power dissipated by the PWM FETs .

3. We assume 1 absorbivity coefficient of the printed boards and 1 emissivity coefficient from the box walls.

4. The printed board cards are thermally connected to the box structure by means of the wedge type “Calmark card-lok” retainers, two per board at the lateral edges of the cards. These card locks guarantee that the heat collected by the copper fingers on the components side and solder side of the CPU and I/F boards is efficiently transmitted to the box walls. Moreover there is a stiffening and heat collecting bar crossing the DC/DC converter board, on which are mounted the power FETs transistors, that is connected to two L-shaped bars in turn connected to the above “Calmark card-lok” retainers so that the heat is efficiently carried to the box walls. (see figure 1, figure 2 and figure 3). In the following analysis we will also neglect the thermal conduction of the stiffening and heat collecting bar to the DC/DC converter board via five fixing screws.

5. The CPU and I/F printed board dimensions are 23.34 x 16.6 cm^2;
   the motherboard dimensions are 23.8 x 23 cm^2;
   the box size is 240 x 258 x 194 mm^3;
   the stiffening and heat collecting bar dimensions are 21.5 x 2 x 0.5 cm^3;
   the L-shaped bars dimensions are 12 x 2.5 x 0.5 and 12 x 1 x 0.5 cm^3.

All power FETs are connected to the stiffening and heat collecting bar and L-shaped lateral bars with total bars surface A_c. Let us suppose that the bars are suspended inside the box, whose temperature is T_s, without any thermal connection to the box itself, and let us calculate their steady state temperature under these worst case conditions.

We have for the bars temperature T_c:

$$T_c = \sqrt[4]{P_i / A_c.s + T_s^4} \quad \text{(K)}$$

where: $s = 5.67x10^{-12}\ J / cm^2$

$A_c =$ bars surface (107.5 + 168 = 275.5 cm^2)

T_c, T_s = temperatures (K); T_s = 45 °C (AD3)

$P_i =$ total power dissipated by the FETs (7.2 W) we obtain T_c = 76 °C.

If the box temperature is T_s = 50 °C (switch-OFF case; AD3), we obtain T_c = 80 °C.

3.3 Conclusions

After considering that:

- we have neglected the heat conduction to the box walls and hence to the S/C structure, i.e. we have neglected the main heat dissipating path;
- we have neglected the thermal conduction of the 5 screws fixing the stiffening bar to the DC/DC printed card, that also contributes to the increase of the A_c area;
- the FETs (2N7224, REF3, REF5) are tightly screwed to the stiffening bar; their junction-to-case thermal resistance is 0.83 °C/W so that their Δ_T is about:

  7.2/2 * 0.83 = 3 °C;

  their case to sink thermal resistance is 0.21 °C/W so their Δ_T is about:

  7.2/2 * 0.21 = 0.76 °C;

by taking into account a non perfect matching between the FETs and the bar (mounting surface non perfectly flat and smooth) and assuming a total Δ_T of 10 °C between FETs and bar (instead of the above computed about 3.76 °C), we would obtain an average FETs temperature not greater than 86 °C, with the box temperature at 45 °C, or not greater than 90 °C, with the box temperature at 50 °C.

We conclude then that in any case the FETs temperatures are well within their 150 °C rated maximum temperatures and from the thermal point of view the design is valid.

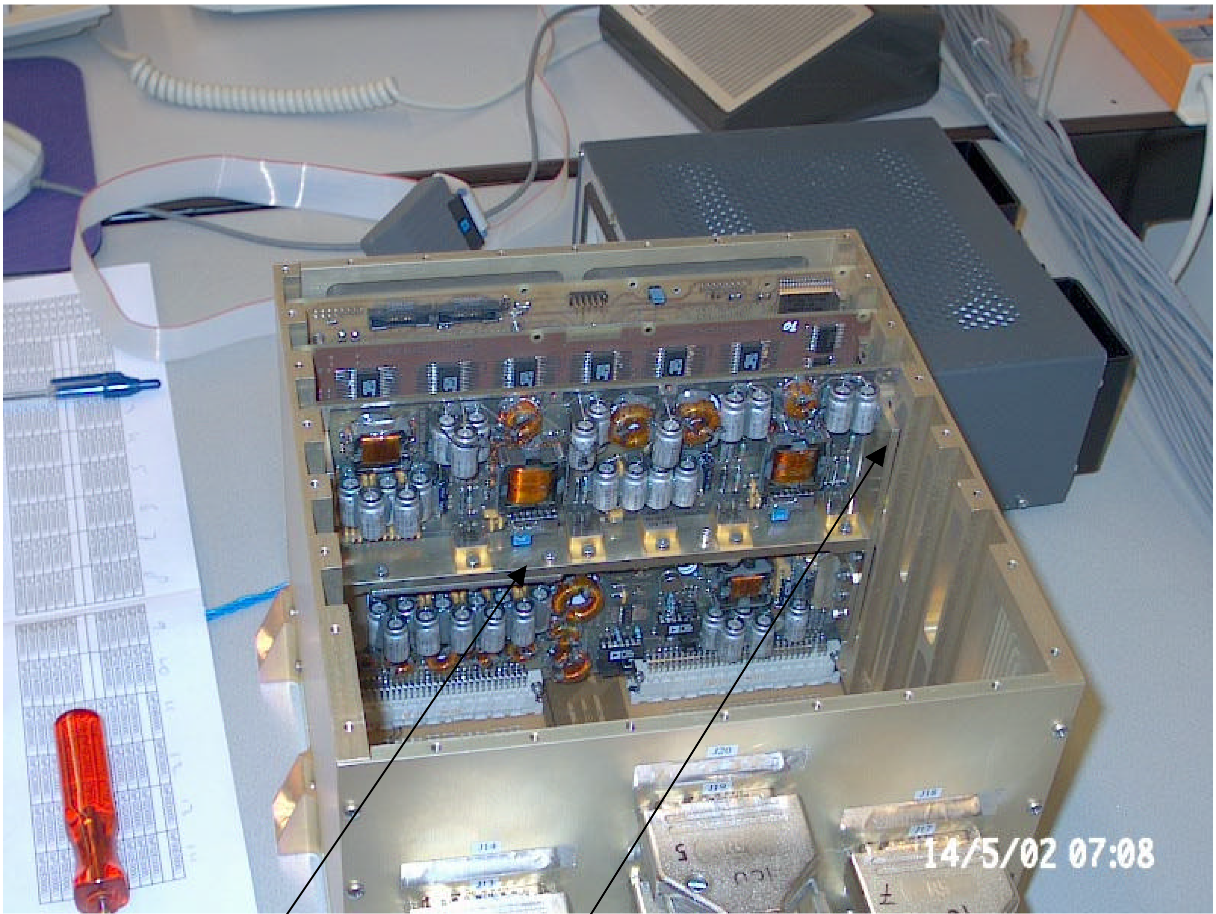

L-shaped lateral bars (2 of) connected to the stiffening bar

Stiffening and heat collecting bar; the "Calmark card-lok" retainers are not visible.

Figure 1

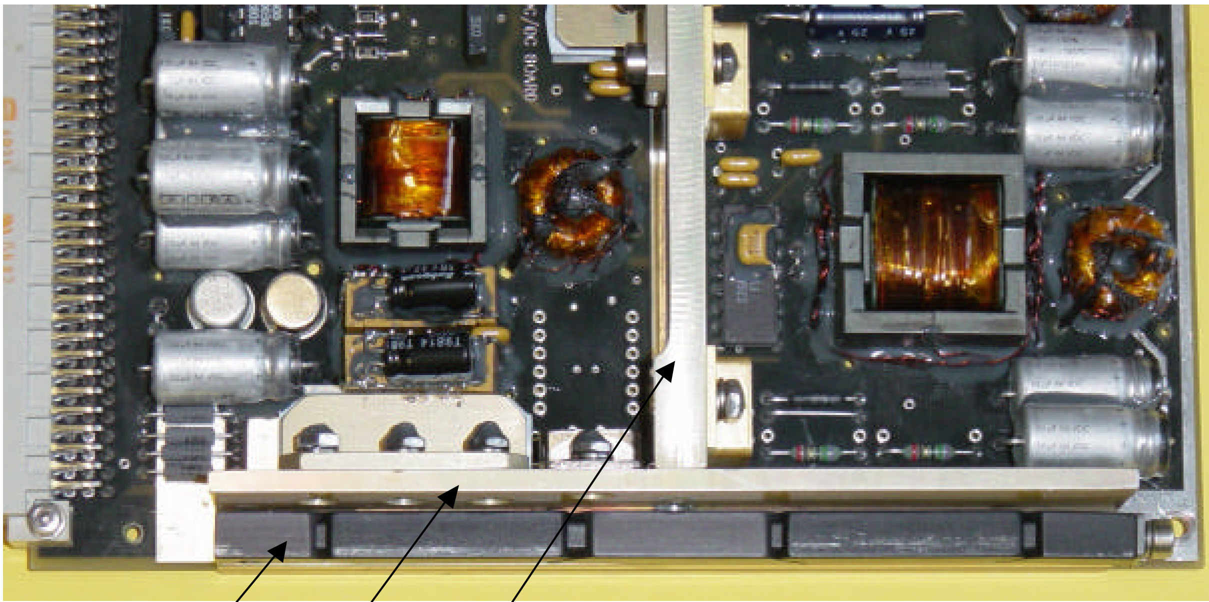

stiffening and heat collecting bar

L-shaped bar

“Calmark- card-lok”

Figure 2

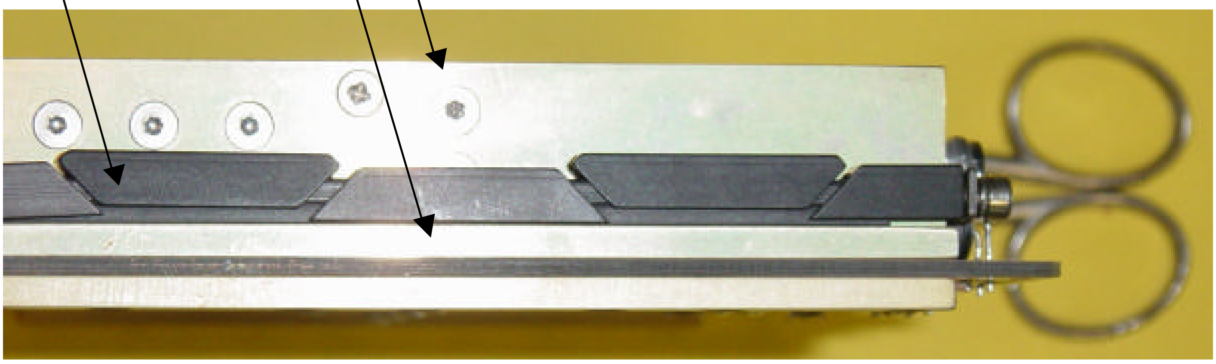

Figure 3 Detail of the “Calmark “card-lok” retainer and of the L-shaped bar

4 Structural Analysis

To simplify the analysis it is considered only the worst case so that all computations are made easy and there is no need of dedicated software programmes, with a lot of dimensions data to be input in order to get in output a simulated stress distribution when applying the vibration levels as defined in AD2.

The electronics boards inside the box are firmly kept in place by:

- 2 large connectors connected to the motherboard, in turn screwed to the box base plate;
- 2 “Calmark “card-lok” retainers connected to the box lateral walls;
- an appropriate comb-like bar connected to the box cover;
- a board stiffener placed nearly at the centre of the board and connected to the board itself by means of 5 screws.

We are not analytically checking then the integrity of the boards when submitted to the stress induced by the vibrations as they are considered firm in place (see figures 1, 2 and 3).

To our purposes it is important to check that no damage is sustained by the DPU structural box when the stress applied on a single box foot, both in bending moment and in shear stress components, is duly incremented by the maximum acceleration to which the box is exposed during the qualification vibration tests.

4.1 Bending Moment check

The box is provided with 6 feet, our analysis is considering the stress applied as a bending moment when one foot is out of order for whatever reason and all the box weight is sustained by 5 feet. We consider one of the remaining 5 feet as a cantilever beam with the load applied to the centre of the fixation screw. The applied load is multiplied by 25 as 25 g (AD2) is the maximum acceleration level to which the box is subjected during sinusoidal vibration tests,(see the following figure).

a = 4 mm

b = 22 mm

d = 8 mm

P = 7.6/5 Kg

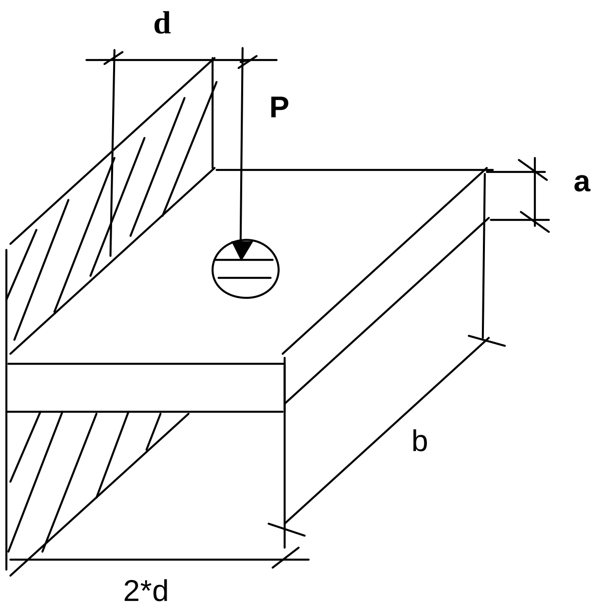

Under these conditions the stress due to the bending moment σ has to be lower than the *yield strength* (maximum elastic deformation) R_p, typical of the used material (Al alloy 6082), divided by the safety factor γ:

$\sigma < R_p/\gamma$

We have for the bending moment:

σ = P* d/W = 50.8 N/mm^2 (or MPa)

where:

P = 7.6 Kg*25/5 = 373 N (box weight divided by 5 feet at 25 g times the gravity acceleration);

W = a^2 * b/6 = 58.7 mm^3 is the *section modulus*.

We obtain then

$\sigma < R_p/\gamma = 50.8 < 110$ N/mm^2 the right hand side term being the Al alloy R_p.

The γ safety factor is larger than 2.

4.2 Shear check

The shear check considers the same box foot and checks for the shear applied to the foot to be as follows:

$\tau < R_p / 2*\gamma$ Tresca's (or Guest's) criterion

where $\tau = 3*P/2*A$; A is the foot section a*b and P is as above

We obtain for $\tau = 6.4$ N/mm^2

The value obtained for τ should be as follows:

$\tau = 6.4 < 110/2*\gamma$

The γ safety factor is hence larger than 8.

4.3 Conclusions

In our assumptions we have for simplicity:

- neglected the two foot ribs, acting as stiffening brackets, that greatly reduce the value of the dimension "d" (see figure 1) notably increasing the foot strength;
- considered the case where one foot, for whatever unknown reason, is not connected any more to the S/C structure, leaving only 5 feet to support the stresses induced by the S/C vibration.

- Considered a weight of 7.6 kg instead of the expected 7.2.

Also after this worsening simplifications we obtain in the two analysed cases safety factors of 2 for the bending moment case and of more than 8 for the shear case.

We conclude then that in any case the box feet are adequate to support, with appropriate margins, the mechanical stresses induced by the vibrations and from the mechanical point of view the design is valid.